IJCRT.ORG ISSN : 2320-2882

INTERNATIONAL JOURNAL OF CREATIVE RESEARCH THOUGHTS (IJCRT)

An International Open Access, Peer-reviewed, Refereed Journal

# SURFACE FUNCTIONALIZED NANOCOMPOSITE $Zr_{(0.25)}Sn_{(0.75)}O_4$ THICK FILMS FOR THE DETECTION OF PPM LEVEL $H_2S$ GAS OPERABLE AT ROOM TEMPERATURE

**G. B. Shelke**

Associate Professor, Dept. of Physics, Nanasaheb Y. N. Chavan College, Chalisgaon, MS, India, 424101

***Abstract:*** It is observed that, pure stoichiometric $SnO_2$ and $ZrO_2$ powders are expected to be insulating in nature. However, synthesized powders of bulk $SnO_2$ and $ZrO_2$ are not exactly stoichiometric and hence not insulating. Bulk tin oxide and zirconium oxide powders were observed to be less sensitive to polluting gases. So, nanostructured tin oxide and zirconium oxide powders were synthesized by disc type ultrasonicated microwave assisted centrifuge technique. Nanocomposite material, $Zr_{(0.25)}Sn_{(0.75)}O_4$ was prepared by using synthesized $ZrO_2$ and $SnO_2$ powders by taking their 1:3 proportion. Thick films of nanostructured pure $Zr_{(0.25)}Sn_{(0.75)}O_4$ powder were fabricated by screen printing technique. These films were surface functionalized by strontium oxide for different intervals of time followed by firing at 450°C for 30 min The characterizations of the unmodified and surface activated nanostructured $Zr_{(0.25)}Sn_{(0.75)}O_4$ powder by $SrO_2$ have been investigated by FESEM, E-DAX, XRD, etc. Electrical and gas sensing performance of the thick films were also studied in the laboratory.

***Keywords:*** **$Zr_{(0.25)}Sn_{(0.75)}O_4$, Surface activation by $SrO_2$, Thick films, Characterizations, etc.**

## I. INTRODUCTION

The concentration of the gas in the environment which produces an undesirable and disastrous change in the physical, chemical or biological characteristics of air, soil and water that can harmfully affect the living beings is called as pollution. Heavy industrialization, uncontrolled urbanization and careless application of technology can cause pollution [1-5]. There are three major types of pollution, viz. air pollution, water pollution and soil pollution. Out of these, air pollution is a major threat for modern society. Current burning issues are global warming, the cruelest episodes like Bhopal gas tragedy, leakage from the Ukraine atomic reactor plant, blackening of world heritage places like Taj Mahal and Ajanta caves are the effects of air pollution. Along with this, some domestic threats are also occurring all over the world. The main culprits behind all such hazards are the toxic, inflammable and explosive gases. Gases play the key role in many industrial or domestic activities. In the last twenty years, the demand for gas detection and monitoring has increased. Particularly, the awareness of the need to protect the environment has grown. This century is the century of automation. It requires fast, simple, safety control and reliable measurement technology of the physical quantities [6].

The aim of the present work is, to fabricate and develop the gas sensors by utilizing the pure and surface activated $SnO_2$-$ZrO_2$ nanocomposites so that, they could be able to detect various gas traces (ppm / ppb).

## II. OBJECTIVES

i. To synthesize the nanostructured $SnO_2$ and $ZrO_2$ by one of the simplest and cheapest process known as disc type ultrasonicated microwave assisted centrifuge technique.
ii. To prepare a nanocomposite material, $Zr_{(0.25)}Sn_{(0.75)}O_4$ using $ZrO_2$ and $SnO_2$ synthesized materials by taking their 1:3 proportion.

iii. To prepare the thick films of nanostructured $Zr_{(0.25)}Sn_{(0.75)}O_4$ by screen printing technique. This is one of the simplest and low cost technique.
iv. To ensure longer life by maintaining proper thixotropy and rheology of the thick films.
v. To achieve a suitable surface functionalization (activation) by dipping the thick films of $Zr_{(0.25)}Sn_{(0.75)}O_4$ in to $SrO_2$ for enhancing the gas response and selectivity.
vi. To analyze the synthesized pure and modified materials by different characterization techniques.
vii. To investigate the electrical and gas sensing performance of pure and surface activated $Zr_{(0.25)}Sn_{(0.75)}O_4$ thick films.
viii. To study the active, selective, long term stable and response - recovery natures of the $Zr_{(0.25)}Sn_{(0.75)}O_4$ thick films.

## III. Material and Methods

### A) Synthesis of $Zr_{1-x}Sn_xO_4$ Nanocomposite Powders

$Zr_{1-x}Sn_xO_4$ nanocomposites in the form of dry powders were synthesized by disc type ultrasonicated microwave treatment followed centrifuge technique [7-11], by hydrolysis of AR grade zirconium oxychloride and tin chloride in aqueous-alcohol solution. Initially, aqueous-alcohol solution was prepared from distilled water and propylene glycol in the ratio of 1:1. The prepared solution was then mixed with 1M aqueous solution of zirconium oxychloride and tin chloride in the desired proportions. The special arrangement was made to add drop wise aqueous ammonia at the rate of 0.1 ml / min with constant stirring until the optimum pH of solutions become in the range from 7.9 to 10.8, varies for various concentrations of dopant. After complete precipitation and centrifugation, the hydroxide was washed with distilled water until chloride ions were not detected by $AgNO_3$ solution. Then the precipitates were allowed for ultrasonication and then placed in a microwave oven for 10 minutes with continuous on-off cycles, periodically, followed by calcination at 500°C for 2 hrs. in muffle furnace. The dried precipitates were ground by agate pestle-mortar to ensure sufficiently fine particle size and re-calcined in a muffle furnace at 500°C for 2 hrs., to eliminate the organic impurities, if present. The crystallite size of synthesized nanocomposites was monitored by XRD analysis and confirmed on calculating by Scherer's formula. Thus, the dry powders of nanostructured $Zr_{(0.25)}Sn_{(0.75)}O_4$ have been prepared and ready to use.

### B) Thick Film Fabrication

The thixotropic paste of $Zr_{1-x}Sn_xO_4$ (1-x = 0.25 and x = 0.75) was formulated by mixing the synthesized nanostructured powder of pure $ZrO_2$ and pure $SrO_2$ with a solution of ethyl cellulose (a temporary binder) in a mixture of organic solvents such as butyl cellulose, butyl carbitol acetate and turpineol. The ratio of inorganic to organic part was kept as 80:20 while formulating the paste. The thixotropic paste was screen printed on the glass substrates and the thick films of desired patterns were obtained [12-15]. Films prepared were dried at 80°C under an IR lamp, followed by firing at 500°C for 30 min in an ambient air. Silver contacts were made by vacuum evaporation for electrical measurements and monitoring the gas sensing performance of the thick films. Thus, the thick films of pure $Zr_{(0.25)}Sn_{(0.75)}O_4$ are now ready to use in the gas sensing applications.

### C) Surface Functionalization (Activation) of the Thick films

Thick films of $Zr_{1-x}Sn_xO_4$ nanocomposites were fabricated by screen printing technique. The films prepared were fired at 500°C for 30 min in muffle furnace. Then the dried films were surface functionalized (activated) by dipping them into 0.01 M aqueous solutions of strontium chloride for different intervals of time viz. 5 min, 15 min, 30 min and 45 min and dried at 80°C under an IR lamp, followed by firing at 500°C for 30 min in ambient air. The particles of strontium chloride dispersed on the film surface would be transformed to strontium oxide ($SrO_2$), upon firing process. Thus, sensor elements with different mass % of $SrO_2$ incorporated in to thick films of pure $Zr_{1-x}Sn_xO_4$ (1-x = 0.25 and x = 0.75) were prepared. Silver contacts were made by vacuum evaporation for electrical measurements and monitoring the gas sensing performance of thick films [16-18].

## IV. Material Characterizations

### A) Structural Properties (X-Ray Diffraction Studies)

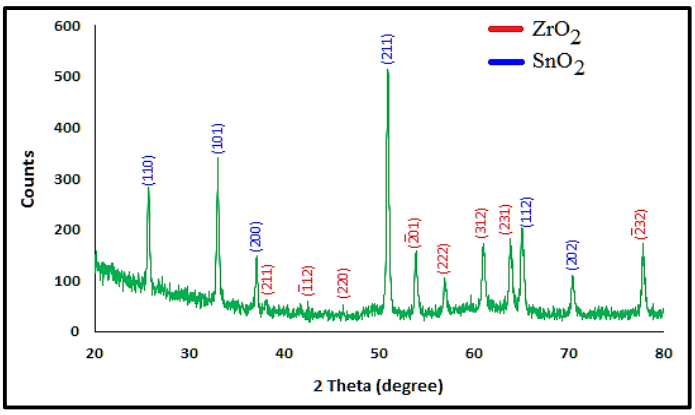


**Fig. 1:** XRD of pure $Zr_{(0.25)}Sn_{(0.75)}O_4$ powder

Fig. 1 depicts the X-ray diffractogram of pure $Zr_{(0.25)}Sn_{(0.75)}O_4$ powder. The 2θ peaks observed are correspond to the (110), (101), (200), (211), ($\bar{1}$12), (220), (211), (201), ($\bar{2}$22), (312), (231), (112), (202) and ($\bar{2}$32) planes of reflections. No peaks corresponding to $SrO_2$ were observed in XRD pattern of surface activated thick films, which may be due to their very small mass % dispersed on the surface of $Zr_{(0.25)}Sn_{(0.75)}O_4$ film. The XRD spectrum reveals that, the material is poly-nano-crystalline in nature and combination of tetragonal-monoclinic in structure. The observed peaks are matching well with JCPDS reported data of pure $SnO_2$-$ZrO_2$. The average crystallite size was observed to be of 8.1 nm and determined using Scherer's formula. It was also observed from XRD that, the synthesized pure $Zr_{(0.25)}Sn_{(0.75)}O_4$ powder has less amorphous nature (26.9%) and more crystalline nature (73.1%), as shown in Table 1.

**Table 1:** Percentage crystallinity and amorphous nature of $Zr_{1-x}Sn_xO_4$ synthesized powder

| Material / Nanocomposite | Crystallinity (%) | Amorphous (%) |
|---|---|---|
| $Zr_{(0.25)}Sn_{(0.75)}O_4$ | 73.1 | 26.9 |

### B) Energy Dispersive Analysis by X-Rays (E-DAX)

**Table 2:** Elemental analysis of pure and $SrO_2$ activated $Zr_{(0.25)}Sn_{(0.75)}O_4$ thick films

| Mass % | Activation Time (min) | | | | | |
|---|---|---|---|---|---|---|
| | 0 (Pure) (Expected) | 0 (Pure) (Observed) | 5 | 15 | 30 | 45 |
| O | 36.40 | 24.72 | 17.19 | 21.40 | 23.56 | 06.36 |
| Zr | 12.97 | 21.30 | 01.55 | 02.42 | 02.51 | 18.65 |
| Sn | 50.63 | 53.98 | 81.18 | 76.07 | 71.71 | 74.53 |
| $Zr_{(0.25)}Sn_{(0.75)}O_4$ | 100 | 100 | 99.89 | 99.85 | 96.96 | 99.37 |
| Sr | 00 | 00 | 00.08 | 00.11 | 02.23 | 00.46 |
| $SrO_2$ | 00 | 00 | 00.11 | 00.15 | 03.04 | 00.63 |
| $SrO_2$ + $Zr_{(0.25)}Sn_{(0.75)}O_4$ | 100 | 100 | 100 | 100 | 100 | 100 |

The quantitative elemental composition of the pure $Zr_{(0.25)}Sn_{(0.75)}O_4$ and $SrO_2$ activated $Zr_{(0.25)}Sn_{(0.75)}O_4$ thick films were analyzed using an energy dispersive spectrometer and mass % of O, Zr, Sn, $Zr_{(0.25)}Sn_{(0.75)}O_4$, Sr, $SrO_2$ and $SrO_2$- $Zr_{(0.25)}Sn_{(0.75)}O_4$ are represented in Table 1. Stoichiometrically expected mass % of O, Zr and Sn (in $Zr_{(0.25)}Sn_{(0.75)}O_4$) are 36.40, 12.97 and 50.63 respectively. However, the observed mass % of the respective elements are 24.72, 21.30 and 53.98 respectively. Thus, the prepared powder of pure $Zr_{(0.25)}Sn_{(0.75)}O_4$ is deficient in oxygen, which increases its n-typeness characteristic. This leads to n-type semiconducting nature of the synthesized $Zr_{(0.25)}Sn_{(0.75)}O_4$. Also, the mass % of Zr, Sn and O in each activated samples are not as per the stoichiometric proportion and all samples are observed to be oxygen deficient. This enhances n-typeness of activated $Zr_{(0.25)}Sn_{(0.75)}O_4$ thick films.

It is clear from Table 2 that, the mass % of $SrO_2$ ($Zr_{(0.25)}Sn_{(0.75)}O_4$) on the surface of the film increases (decreases) with activation time (except 45 min sample), which may be attributed to the chemisorption of strontium chloride particles on the surface of the thick films proving activation of the film during dipping process. This forms p-$SrO_2$ / n-$Zr_{(0.25)}Sn_{(0.75)}O_4$ heterojunctions on the surface of the film, leading to increase the resistivity.

### C) Microstructural Analysis (SEM)

#### i) Pure $Zr_{(0.25)}Sn_{(0.75)}O_4$

Fig. 2 depicts the SEM image of pure $Zr_{(0.25)}Sn_{(0.75)}O_4$ thick film fired at 500°C for 30 min, which consists of voids and a wide range of randomly distributed grains with sizes ranging from 10 nm to 30 nm. The film has porous nature, which supports the adsorption-desorption type of gas sensing mechanism. The nanoscaled grains exhibit high surface to volume ratio. The less numbers of smaller grains of zirconium oxide are fused with the large numbers of larger grains of tin oxide.

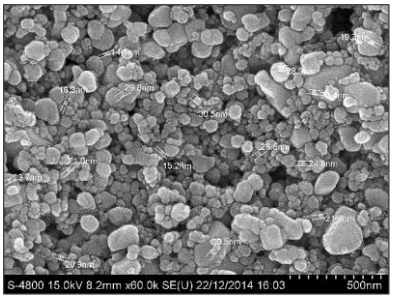


**Fig. 2:** Micrograph of pure $Zr_{(0.25)}Sn_{(0.75)}O_4$ thick film

**ii) $SrO_2$ Activated $Zr_{(0.25)}Sn_{(0.75)}O_4$**

Figs. 3 (a to d) depicts the microstructures of $SrO_2$ activated $Zr_{(0.25)}Sn_{(0.75)}O_4$ thick films activated for 5 min, 15 min, 30 min and 45 min, respectively. The films consist of smaller grains of $SrO_2$ associated with the larger (agglomerated) grains of $Zr_{(0.25)}Sn_{(0.75)}O_4$. The film activated for 15 min exhibits larger response to $H_2S$ gas at room temperature as well as at 50°C. Due to nanoscale structure, the effective surface to volume ratio is large, which enhances the gas response. The films consist of voids, having grain sizes ranging from 10 nm to 30 nm distributed non-uniformly. It was also observed that, the mass percentage of $SrO_2$ increases with activation time. The films activated for 30 min and 45 min exhibits less response as compared with the film activated for 15 min. It may be due to the large numbers of $SrO_2$ particles dispersed on the surface of the film, reduces the surface to volume ratio.

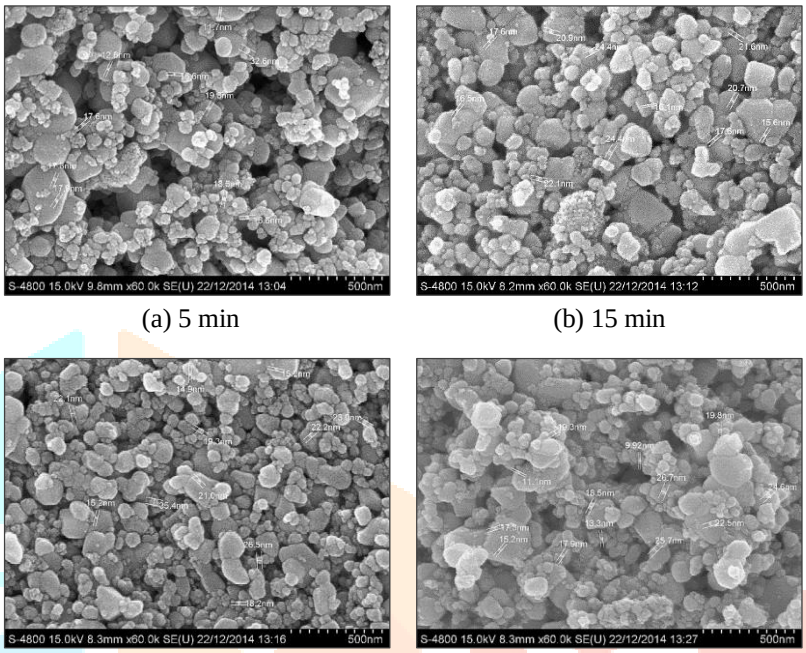


(a) 5 min (b) 15 min

(c) 30 min (d) 45 min

**Fig. 3:** Micrographs of $SrO_2$ activated $Zr_{(0.25)}Sn_{(0.75)}O_4$ thick films

## V. ELECTRICAL CHARACTERIZATIONS

### A) I-V Characteristics

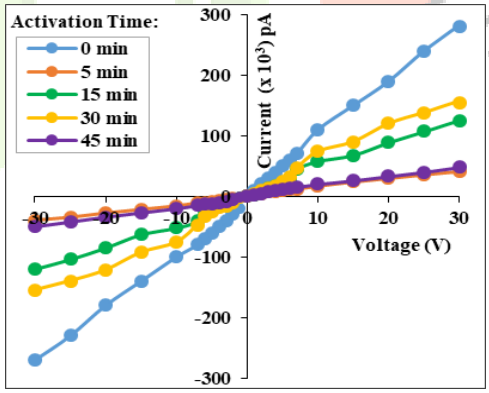


**Fig. 4:** I-V characteristics of $SrO_2$ activated $Zr_{(0.25)}Sn_{(0.75)}O_4$ thick films

Fig. 4 depicts the I-V characteristics of pure and $SrO_2$ activated $Zr_{(0.25)}Sn_{(0.75)}O_4$ thick films. It is clear from the symmetrical nature of I-V characteristics that, the material as well as silver contacts made on the films for external connections, are ohmic in nature. The material is therefore said to have possessing the resistive properties, though more or less.

**B) Electrical Conductivity**

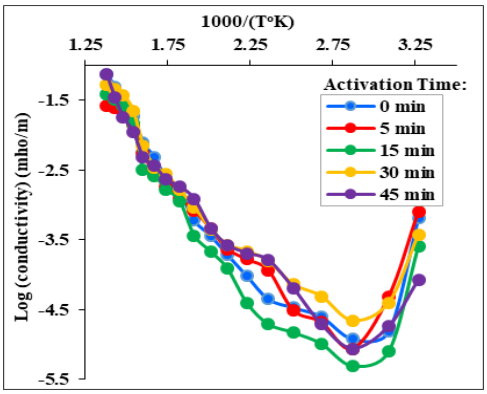


**Fig. 5:** Conductivity profile of $SrO_2$ activated $Zr_{(0.25)}Sn_{(0.75)}O_4$ thick films

Fig. 5 depicts the variation of log of conductivity with the reciprocal of operating temperature of $SrO_2$ activated $Zr_{(0.25)}Sn_{(0.75)}O_4$ thick films. The conductivities of all the samples are minimum at 75°C operating temperature. It was found that, all the pure and activated films exhibit the lowest conductivities (nearly linear) in the temperature range from 100°C to 75°C. This is the temperature range in which all the films exhibit insulating nature, above which the films exhibit NTC and below it, the films exhibit PTC nature. Thus the material switches its semiconducting nature from NTC to PTC through insulating nature, with decrease in temperature from 400°C to room temperature (32°C). So, the temperature range from 100°C to 75°C is the notch for which the material exhibits insulating property. Hence, one should not expect the application of this material in the field of gas sensing or any optoelectronic fields in this temperature range. The experimental observations of gas sensing support this statement.

This may be attributed to the fact that, at room temperature, pure $Zr_{(1-x)}Sn_{(x)}O_4$ is deficient in oxygen, more or less, exhibiting the n-type semiconducting nature. But, as the temperature increases, slowly up to 75°C, the oxygen gets adsorbed on the material. Due to oxygen adsorption, the n-typeness of the material decreases slowly and the material tries to achieve the stoichiometric proportion of oxygen travelling towards insulating nature, perfectly at 75°C and up to 100°C. Above 100°C, the material again disturbs its stoichiometry by losing the oxygen, exhibiting the n type semiconducting nature ultimately, increasing the conductivity with temperature.

## VI. GAS SENSING PERFORMANCE

### A) Pure $Zr_{(0.25)}Sn_{(0.75)}O_4$

#### 1) Gas Sensing Response of Pure $Zr_{(0.25)}Sn_{(0.75)}O_4$

Fig. 6 shows the variation of $H_2S$ and LPG (500 ppm each) gas response of pure $Zr_{(0.25)}Sn_{(0.75)}O_4$ thick films with operating temperature. The maximum responses to $H_2S$ and LPG obtained are of the order of 32 and 23 at room temperature and at 150°C, respectively. Upon exposure of $H_2S$ gas, the material $Zr_{(0.25)}Sn_{(0.75)}O_4$ gets converted to SnS and hence increasing the conductivity of the material at low temperature. However, as the temperature increases, SnS gets oxidized decreasing the $H_2S$ gas response.

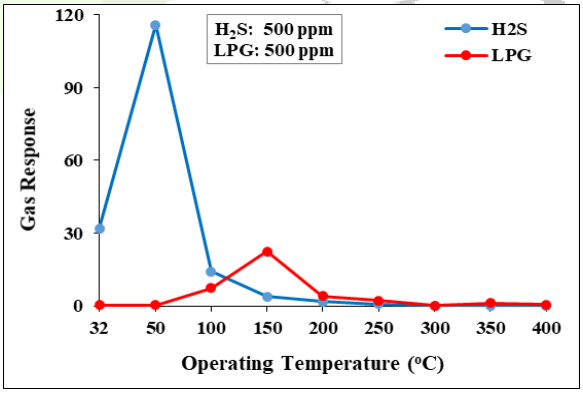


**Fig. 6:** $H_2S$ and LPG response of pure $Zr_{(0.25)}Sn_{(0.75)}O_4$ thick film

**2) Selective Nature of Pure $Zr_{(0.25)}Sn_{(0.75)}O_4$**

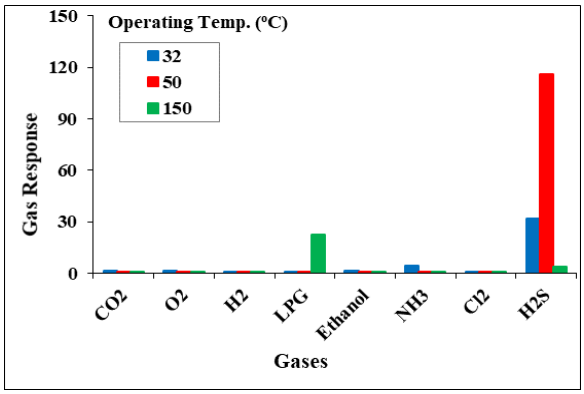


**Fig. 7:** Selective nature of pure $Zr_{(0.25)}Sn_{(0.75)}O_4$ thick film

Fig. 7 shows the selective nature of pure $Zr_{(0.25)}Sn_{(0.75)}O_4$ thick film to $H_2S$ and LPG gases. The sensor is highly selective to $H_2S$ and LPG against different gases, viz. $CO_2$, $O_2$, $H_2$, Ethanol, $NH_3$ and $Cl_2$ at different operating temperatures.

**B) $SrO_2$ Functionalized $Zr_{(0.25)}Sn_{(0.75)}O_4$**

**1) Gas Sensing Response of $SrO_2$ Activated $Zr_{(0.25)}Sn_{(0.75)}O_4$**

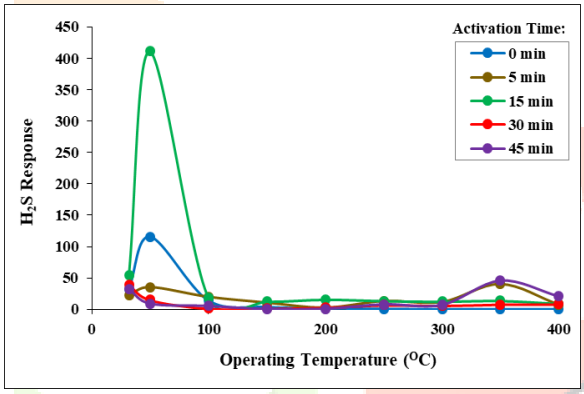


**Fig. 8:** $H_2S$ response of pure and $SrO_2$ activated $Zr_{(0.25)}Sn_{(0.75)}O_4$ thick films

Fig. 8 depicts the variation of 5 ppm $H_2S$ gas response with operating temperature of pure and $SrO_2$ activated $Zr_{(0.25)}Sn_{(0.75)}O_4$ thick films. It is clear from figure that, $SrO_2$ activated $Zr_{(0.25)}Sn_{(0.75)}O_4$ thick films at 15 min activation time gives highest response to 5 ppm $H_2S$ gas at room temperature (32°C) as well as at 50°C operating temperature. From elemental analysis, it is observed that, the $SrO_2$ activated $Zr_{(0.25)}Sn_{(0.75)}O_4$ (15 min) thick film is observed to be oxygen deficient. This enhances n-typeness of activated $Zr_{(0.25)}Sn_{(0.75)}O_4$ film. During surface activation of the film, p-$SrO_2$ / n-$Zr_{(0.25)}Sn_{(0.75)}O_4$ heterojunctions were formed, decreasing the conductivity of the activated surface of the film. Upon exposure of $H_2S$ gas, the n-typeness of $Zr_{(0.25)}Sn_{(0.75)}O_4$ decreases and enhances p-typeness in the extent that ruptures the p-n heterojunctions and the whole material exhibits p-type semiconductivity. The holes contribute the net flow of current in the surface of the material. This may be the reason of increase in conductivity of the sensor upon exposure of $H_2S$ at room temperature. $H_2S$ response increases up to 50°C and decreases further with increase in operating temperature.

**2) Active and Selective Nature**

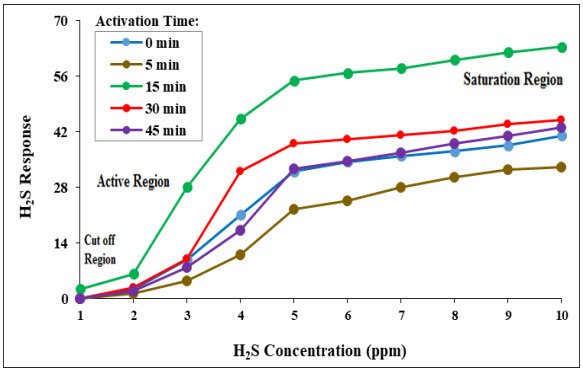


**Fig. 9:** Variation in $H_2S$ response

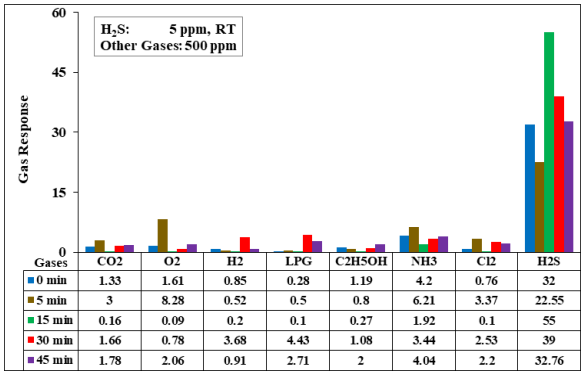


| Gases | CO2 | O2 | H2 | LPG | C2H5OH | NH3 | Cl2 | H2S |
|---|---|---|---|---|---|---|---|---|
| 0 min | 1.33 | 1.61 | 0.85 | 0.28 | 1.19 | 4.2 | 0.76 | 32 |
| 5 min | 3 | 8.28 | 0.52 | 0.5 | 0.8 | 6.21 | 3.37 | 22.55 |
| 15 min | 0.16 | 0.09 | 0.2 | 0.1 | 0.27 | 1.92 | 0.1 | 55 |
| 30 min | 1.66 | 0.78 | 3.68 | 4.43 | 1.08 | 3.44 | 2.53 | 39 |
| 45 min | 1.78 | 2.06 | 0.91 | 2.71 | 2 | 4.04 | 2.2 | 32.76 |

**Fig. 10:** Selective nature

The variation of $H_2S$ response of pure and $SrO_2$ activated $Zr_{(0.25)}Sn_{(0.75)}O_4$ thick films with $H_2S$ gas concentration at room temperature, are represented in Fig. 9. It is clear from figure that; the gas response goes on increasing linearly with gas concentration up to 5 ppm. The rate of increase in $H_2S$ response was relatively larger up to 5 ppm and saturated beyond 5 ppm. Hence, the active region of the sensor would be up to 5 ppm.

It is observed from Fig. 10 that, the 15 min $SrO_2$ activated $Zr_{(0.25)}Sn_{(0.75)}O_4$ thick film is most sensitive to 5 ppm $H_2S$ at room temperature. This is the optimized condition as far as surface activation of $Zr_{(0.25)}Sn_{(0.75)}O_4$ with the help of $SrO_2$ is concerned. Also, it has high selectivity against different gases, viz. carbon dioxide, oxygen, hydrogen, liquefied petroleum gas, ethanol, ammonia and chlorine.

### 3) Long Term Stable and Response - Recovery Nature

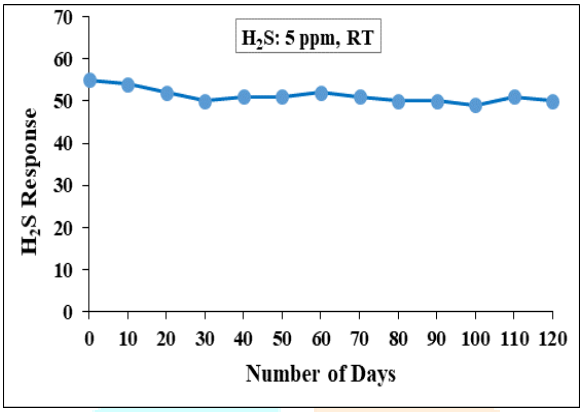


**Fig. 11:** $H_2S$ response over long time duration (Days)

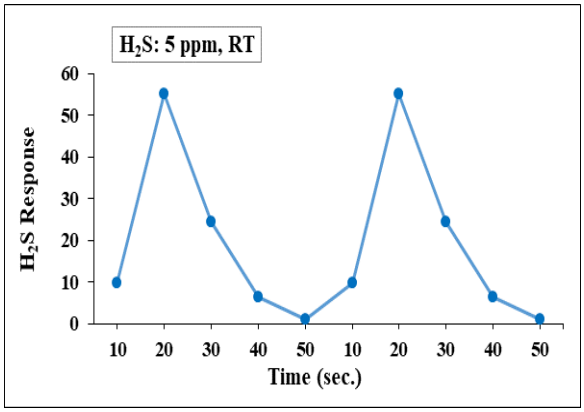


**Fig. 12:** Response and recovery nature

Fig. 11 indicates the $H_2S$ response over a long time duration for the $SrO_2$ activated $Zr_{(0.25)}Sn_{(0.75)}O_4$ (15 min) thick film sensor. The sensor was observed to be the most sensitive to $H_2S$ at room temperature. The sensor response to $H_2S$ was observed to be constant over a long duration (few months). It was observed that, the sensor response decreases by about 10 % after 30 days, and remains same thereafter. This proves the long term stability of the sensor.

The response and recovery of the $SrO_2$ activated $Zr_{(0.25)}Sn_{(0.75)}O_4$ (15 min) thick film sensor is represented in Fig. 12. The response time of the sensor was of the order of 15 sec. to 5 ppm of $H_2S$ gas and recovery time is of the order of 22 sec. For better performance of the sensor, the recovery should be very fast. When the gas exposure was switched off, the sensor returned back to its original chemical status, within a very short time (~22 sec.). This is the main feature of this sensor.

## VII. Conclusions

1. Disc type ultrasonicated microwave assisted centrifuge technique is one of the simplest and cheapest method to synthesize the nanostructured $SnO_2$ and $ZrO_2$.
2. Thick films fabrication by screen printing technique is one of the simplest and low cost technique.
3. Surface functionalization (activation) by dipping the thick films of $Zr_{(0.25)}Sn_{(0.75)}O_4$ in to $SrO_2$ is very useful for enhancing the gas response and selectivity.
4. From the results obtained, some important conclusions made for the gas sensing performance of the sensor.
5. 15 min $SrO_2$ activated $Zr_{(0.25)}Sn_{(0.75)}O_4$ was observed highly sensitive and selective to 5 ppm $H_2S$ gas at room temperature.
6. The excellent features of the sensor are that, it is highly sensitive, selective, low cost, portable in size and weight, long term stability, fast response and quick recovery.

## Acknowledgements

Author is grateful to the research supervisor Dr. D. R. Patil, Bulk and Nanomaterials Research Lab., Rani Laxmibai College Parola, Chairman of Sahjivan Shikshan Prasarak Mandal Ltd. Tehu, Parola and Principal of the Rani Laxmibai College, Parola for providing laboratory facilities. Author is also very much thankful to the Hon. Chairman, Secretary and Management of the R. S. S. P. M. Ltd. Chalisgaon as well as to the Principal and Colleagues of Nanasaheb Y. N. Chavan College, Chalisgaon.

## References

[1] Dasmann R. F., Environmental conservation, 4th Ed., John Wiley and Sons, Inc., New York 1976; p. 310-338.
[2] Moore P. D., Pollution: Too much of a good thing, Nature (London) 1995; 374: p. 117-118.
[3] Brooks M., Coghlan A., Live and let live, New Scientists 1998; p. 46-49.
[4] Durham W. B., Industrial Pollution, Sax, N. I., Van Nostrand Reinhold Co., New York 1974; p. 10-35.
[5] Eckerman I., Bhopal Gas Catastrophe 1984: Causes and Consequences, Encyclopedia of Environmental Health 2011; p. 302-316.
[6] Patil D. R., Everyman's Science, J. Indian Science Congress Association, 2011; XLVI No. 3: p. 155-161.
[7] Gawas U. B., Verenkar V. M. S., Patil D. R., Nanostructured ferrite based electronic nose sensitive to ammonia at room temperature, Sens. Transducers 2011; 134: p. 45-55.

[8] Kapse S. D., Raghuwanshi F. C., Kapse V. D., Patil D. R., Characteristics of high sensitivity ethanol gas sensors based on nanostructured spinel $Zn_{1-x}Co_xAl_2O_4$, J. Current Appl. Phys. 2012; 12: p. 307-312.
[9] Khamkar K. A., Bangale S. V., Dhapte V. V., Patil D. R., Bamne S. R., A Novel Combustion Route for the Preparation of Nanocrystalline $LaAlO_3$ Oxide Based Electronic Nose Sensitive to $NH_3$ at Room Temperature, Sens. Transducers 2012; 146: p. 145-155.
[10] Patil Snehal D., Patil Y. B., Patil D. R., Patel Shahera S., Particle Size Dependent Gas Sensing Performance of ZnO Nanorods based Thick Film Resistors, Intern. J. on Recent and Innovation Trends in Computing and Communication 2015; 3 (8): p. 5063-5068.
[11] Shelke G. B., Deshmukh G. D., Patil D. R., Synthesis and Characterizations of Nano Structured $SnO_2$ Thick Films and their Micro Structural Analysis, Int. J. of Current Research 2019; 11 (7): p.5576-5579.
[12] Patil D. R., Patil L. A., Preparation and study of $NH_3$ gas sensing behavior of $Fe_2O_3$ doped ZnO thick film resistors, Sens. Transducers 2006; 70: p. 661-670.
[13] Patil D. R., Patil L. A., Patil P. P., $Cr_2O_3$-activated ZnO thick film resistors for ammonia gas sensing operable at room temperature, Sens. Actuators B 2007; 126: p. 368–374.
[14] Patil D. R., Patil L. A., Ammonia sensing resistors based on $Fe_2O_3$-modified ZnO thick films, Sensors IEEE 2007; 7: p. 434-439.
[15] Bagal L. K., Patil J. Y., Mulla I. S., Suryavanshi S. S., Studies on the resistive response of nickel and cerium doped $SnO_2$ thick films to acetone vapour, Ceramics International 2012; 38: p. 6171-6179.
[16] Dr. Shelke G. B., Dr. Patil D. R., Gas Sensing Performance of Pure and Modified Nanostructured Screen Printed Zirconia Thick Films, Int. J. of Engineering Research & Technology (IJERT) 2019; 08(08): p. 198-202.
[17] Shelke G. B., Patil D. R., Surface functionalized $Zr_{(0.75)}Sn_{(0.25)}O_4$ by $SrO_2$ thick films as $H_2S$ gas sensors, 2nd Int. Conference on Condensed Matter and Applied Physics, Bikaner, India, American Insitute of Physics (AIP) Conf. Proc. 2017; 1953: p. 030270-1 – 030270-4.
[18] Shelke G. B., Patil D. R., Surface activated nanostructured zirconia thick films for the detection of ppm level oxygen gas operable at room temperature, J. of Emerging Technologies and Innovative Research (JETIR) 2020; 07 (04): p. 58-65.